

# Urbach's tail in the absorption spectra of $\text{Cu}_2\text{GeSe}_3$ semiconducting compound

C. Rincón<sup>a,\*</sup>, G. Marciano<sup>a</sup>, S. M. Wasim<sup>a</sup>, G. Marín<sup>b</sup>, M. Villareal<sup>a</sup>, and G. Sánchez Pérez<sup>a</sup>

<sup>a</sup>*Centro de Estudios de Semiconductores, Facultad de Ciencias,  
Universidad de Los Andes, Mérida 5101, Venezuela.*

\**e-mail: cacogus52@gmail.com*

<sup>b</sup>*Laboratorio de Estructura e Ingeniería de Materiales Nanoestructurados,  
Centro de Investigación y Tecnología de Materiales,  
Instituto Venezolano de Investigaciones Científicas, Maracaibo 4011, Venezuela.*

Received 20 July 2018 ; accepted 27 September 2018

In the present work we report on the analysis of the Urbach's tail in pure and Mn-doped  $\text{Cu}_2\text{GeSe}_3$  samples having small deviation from its ideal stoichiometry. It is found that the high values of the phonon energy  $h\nu_p$  involved in the electrons/excitons-phonon interaction in the formation of this tail are due to structural disorder caused by deviation from ideal stoichiometry. Values of  $h\nu_p$  for pure and doped samples were found to be 48, 60 and 81 meV, respectively, whereas the phonon energy for an entirely ordered  $\text{Cu}_2\text{GeSe}_3$  sample was estimated to be about 25 meV.

*Keywords:* Optical absorption; Urbach's tail; ternary compound; structural defects.

PACS: 71.20.Nr; 71.55.Jv; 78.30.Hv.

## 1. Introduction

Ternary compounds of the  $A_2^I B^{II} C_3^{VI}$  family, where  $A = \text{Cu}$  and  $\text{Ag}$ ;  $B = \text{Ge}$ ,  $\text{Sn}$ , and  $\text{Sb}$ ; and  $C = \text{Se}$ ,  $\text{Te}$ , and  $\text{S}$ , as for instance  $\text{Cu}_2\text{GeSe}_3$  and  $\text{Cu}_2\text{SnSe}_3$ , have received considerable attention recently for Thermoelectric (TE) applications [1-7]. However, although the optical properties of these compounds have been analyzed in some detail [8-14], no studies had reported these materials on their optical absorption coefficient  $\alpha$  just below the band edge, where this parameter varies exponentially with photon energy, a behavior which is referred as Urbach's tail [15,16]. Such studies are of significant importance because they give valuable information about the electron-phonon interaction and structural disorder caused by the compositional deviation from the ideal stoichiometry in semiconductors [17-19].

Hence, in the present work we report on the temperature dependence of Urbach's energy in pure and Mn-doped samples of the orthorhombic structure  $\text{Cu}_2\text{GeSe}_3$  compound (CGSe) having small a deviation from the ideal stoichiometry 2:1:3. The results here obtained are analyzed with the theoretical model proposed by Wasim *et al.* [18] and the effect of structural disorder caused by the deviation from ideal molecularity and valence stoichiometry on the phonon energy of pure and Mn-doped CGSe is discussed.

## 2. Crystal growth and Experimental methods

Polycrystalline pure and Mn doped (containing 0.03% Mn in weight) CGSe samples used in the present study were prepared by melting with direct fusion the constituent elements in a sealed and evacuated quartz tube. The ampoules were placed in a vertical furnace. Initially they were heated from room temperature to 300°C at the rate of 30°C/h. The mixture was kept at this temperature for 24 h and then heated

at 6°C/h up to 960°C. Again the mixture was kept at this temperature for 24 h. Then it was heated to 1150°C at the rate of 30°C/h. The mixture in the liquid phase was agitated carefully by periodically rocking the furnace for 48 h. It was cooled at a rate of 60°C/h up to 900°C and then to 800°C at 10°C/h with a dwell time at this temperature of 24 h. The cooling rate from 800 to 650°C was 6°C/h with a dwell time of 24 h. The furnace was then cooled to 500°C at 20°C/h and the ingot was annealed at this temperature for 200 h. Finally, the furnace was cooled to room temperature at 30°C/h.

The chemical composition of samples taken from the central part of the ingots was obtained by energy dispersive X-ray spectroscopy (EDX).

The powder X-ray diffraction (XRD) patterns of the samples were recorded at room temperature using a calibrated Guinier-de Wolf camera. The camera was installed in a x-ray generator equipped with a Cu-target tube operated at 40 kV and 20 mA. The position of each peak was established using the  $\alpha_1$  component ( $\lambda\text{CuK}\alpha_1 = 0.15406 \text{ nm}$ ).

For the measurements of the absorption coefficient spectra at various temperatures, parallel-sided single-crystal samples were selectively cut from polycrystalline ingots grown from the melt as described above. They were placed in a  $\text{He}_2$  cryostat operating in the range from 10 to 300 K. A fully automated SPEX 1870 monochromator and a 170 W tungsten lamp as a light source were used. The transmitted radiation was detected by a cooled PbS detector.

## 3. Theory

At a given temperature, the optical absorption coefficient  $\alpha$  just below the fundamental absorption edge is called Urbach's tail and can be expressed by a relation of the form [15]

$$\alpha(h\nu) = \alpha_0 \exp[\sigma(h\nu - E_0)/K_B T], \quad (1)$$

where  $h\nu$  is the incident photon energy,  $\sigma$  the steepness parameter,  $\alpha_0$  and  $E_0$  two characteristic parameters of the material, and  $K_B$  the Boltzmann constant. This behavior has its origin in the interaction of electrons and excitons with phonons [16,18].  $E_U = K_B T/\sigma$ , which represents the width of the exponential tail, is called Urbach's energy. The steepness parameter  $\sigma$  is found to satisfy the relation [18]

$$\sigma = \sigma_0(2K_B T/h\nu_p) \tanh(h\nu_p/2K_B T), \quad (2)$$

where  $h\nu_p$  is the energy of the phonons associated with Urbach's tail and  $\sigma_0$  a constant. Different values of  $h\nu_p$  for the same material, some of them much higher than the highest optical mode observed in the vibrational spectra of each material, have been reported in ternary chalcopyrite [18,20-22] and chalcopyrite-related structure compounds [23-26].

The existence of these unusually higher energy modes is explained by assuming that they are due to the structural disorder caused by the deviation from ideal molecularity and valence stoichiometry in the samples studied [18]. This is described by means of the parameter  $\Delta Z$  defined as  $\Delta Z = \Delta X + \Delta Y$ , where for the present compound CGSe,  $\Delta X = |\text{Cu}|/|\text{Ge}| - 1$ , and  $\Delta Y = |\text{Se}|/|\text{Metal}| - 1$ , represent the deviations from molecularity and valence stoichiometry, respectively [18]. In these relations,  $|\text{Cu}|$ ,  $|\text{Ge}|$ , and  $|\text{Se}|$  being the average concentrations in atomic percent of the constituent elements in CGSe obtained from the composition analysis. This behavior can be expressed by the relation [18]:

$$h\nu_p(\Delta Z) = h\nu_{p_0} + C\Delta Z, \quad (3)$$

where  $h\nu_{p_0}$  is the average of the phonon energy in an entirely ordered system and  $C$  a constant.

On the other hand, to explain the temperature dependence of Urbach's energy in ternary chalcopyrite and chalcopyrite-related structure compounds, Wasim *et al.* [18] have used an

expression of the form:

$$E_U(T, N, P) = (K_B \Theta / \sigma_0) \times [(1 + P)/2 + N/\{\exp(\Theta/T) - 1\}], \quad (4)$$

where the adjustable parameters  $P$  and  $N$  are related to structural disorder and thermal phonon modification, respectively. In a perfectly ordered system,  $P$  and  $N$  are expected to be zero and unity, respectively.  $N$  is introduced in Eq. (4) to take into account the fact that due to structural disorder only a fraction of the total phonon modes excited at a given temperature can interact with excitons/electrons, and  $\Theta$  is a characteristic lattice temperature related to the mean frequency of phonons in the crystal. It is expected to be of the same order as the Debye temperature  $\Theta_D$ .

## 4. Experimental Results and Discussion

A detailed analysis of the XRD patterns confirms that this material crystallizes in an orthorhombic cell with space group  $Imm2$  ( $C_{2v}^{20}$ ), as reported by Parthé and Garin [27] on the basis of a single-crystal analysis. Typical unit cell constants for pure S1 and S2, and Mn doped S3 CGSe, taken from the central part of the ingots, obtained from the X-ray Ritveld refining are listed in Table I. These are in good agreement with those reported in for this material in Ref. 27.

The chemical analysis of samples taken from the central part of the ingots of S1, S2 and S3 CGSe, performed by EDX, gives chemical compositions of  $|\text{Cu}| : |\text{Ge}| : |\text{Se}| = 28.4:15.0:56.6$ ,  $30.1:17.5:52.4$ , and  $26.3:16.0:57.7$ , in atomic percentage, respectively. These are close to the ideal value 2:1:3. However, all the samples show deviations from its ideal stoichiometry. Thus, all the samples have deficiency of Cu with respect to Ge ( $|\text{Cu}|/|\text{Ge}| \approx 1.64-1.89$ ) and an excess of Se over cations ( $|\text{Se}|/|\text{metal}| \approx 1.10-1.35$ ).

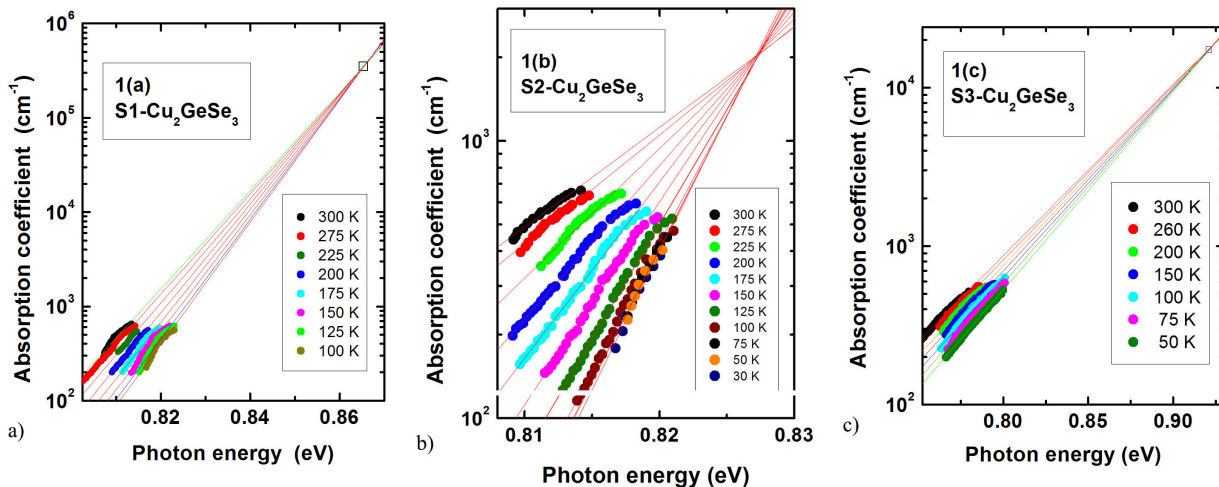


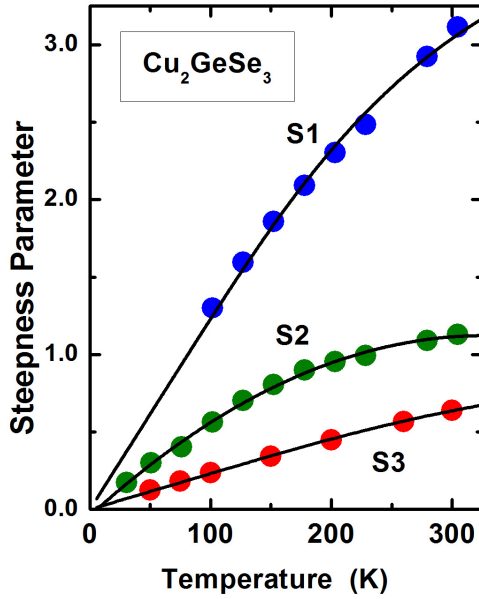
FIGURE 1. Absorption coefficient  $\alpha$  as a function of photon energy  $h\nu$  at different temperatures for pure S1 and S2, and Mn doped S3  $\text{Cu}_2\text{GeSe}_3$  samples.

TABLE I. Unit cell constants  $a$ ,  $b$ ,  $c$  and volume  $V$  for Pure S1 and S2, and Mn-doped S3  $\text{Cu}_2\text{GeSe}_3$  samples.

CGSe-sample	$a$ (nm)	$b$ (nm)	$c$ (nm)	$V$ ( $\text{nm}^3$ )
S1-CGSe	1.1854(4)	0.3954(2)	0.5489(1)	0.2573(2)
S2-CGSe	1.1860(3)	0.3960(1)	0.5475(1)	0.2572(2)
S3-CGSe	1.1864(2)	0.3951(1)	0.5489(1)	0.2573(1)

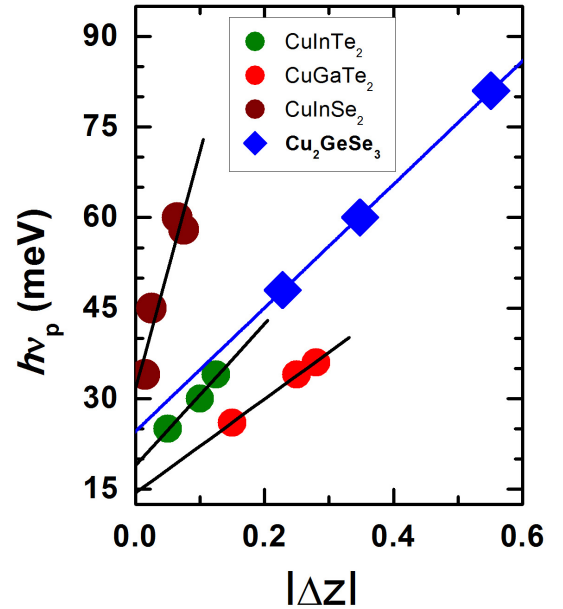
TABLE II. The parameters  $E_0$ ,  $\alpha_0$ ,  $\sigma_0$ , phonon energy associated with Urbach's tail  $h\nu_p$ , absolute value of the molecularity  $|\Delta X|$ , deviation from valence stoichiometry  $|\Delta Y|$ ,  $|\Delta Z| = |\Delta X| + |\Delta Y|$ , and the adjustable parameters P and N for pure S1 and S2 and Mn doped S3  $\text{Cu}_2\text{GeSe}_3$  samples.

CGSe Samples	$E_0$ (eV)	$\alpha_0$ ( $10^4 \text{ cm}^{-1}$ )	$\sigma_0$	$h\nu_p$ (meV)	$ \Delta X $	$ \Delta Y $	$ \Delta Z $	P	N
S1	0.865	34.8	4.30	60	0.087	0.261	0.348	3.81	0.46
S2	0.827	0.203	1.55	48	0.130	0.098	0.228	1.81	0.61
S3	0.921	1.73	1.09	81	0.181	0.370	0.551	5.69	0.29

FIGURE 2. The steepness parameter  $\sigma$  as a function of temperature for pure S1 and S2, and Mn doped S3  $\text{Cu}_2\text{GeSe}_3$  samples. The continuous curves represent a fit of Eq. (2) to the data with the adjustable parameters  $\sigma_0$  and  $h\nu_p$  given in Table II.

The logarithmic variation of  $\alpha$  with  $h\nu$  at several temperatures for pure S1 and S2, and Mn doped CGSe samples are plotted in Figs. 1(a), 1(b), and 1(c), respectively. Linear dependence within certain energy range at each temperature that converges to a single point defined by  $E_0$  and  $\alpha_0$ , is observed in these figures. The value of  $E_0$  and  $\alpha_0$ , obtained from the fit of Eq. (1) to the data of these CGSe samples are listed in Table I.

In addition, the temperature dependence of the steepness parameter is plotted in Fig. 2. Values of  $\sigma_0$  and  $h\nu_p$  obtained from a fit of Eq. (2) to the data are also given in Table II.

FIGURE 3. The change in  $h\nu_p$  with  $|\Delta Z|$  for  $\text{Cu}_2\text{GeSe}_3$  of the present work. Values of  $h\nu_p$  vs.  $|\Delta Z|$  for  $\text{CuInTe}_2$ ,  $\text{CuGaTe}_2$ , and  $\text{CuInSe}_2$  chalcopyrite compounds reported in the literature [18,20] are also shown in this figure for comparison. Straight lines represent linear fits to the data. For CGSe, the extrapolation of the straight line to  $|\Delta Z| = 0$  gives  $h\nu_{p0} \approx 25 \text{ meV}$  ( $\approx 201 \text{ cm}^{-1}$ ).

As mentioned above, it was found for ternary chalcopyrite compounds that high values of  $h\nu_p$ , as those at 48, 60 and 81 meV found for CGSe in the present work, appear due to the structural disorder caused by the deviations from molecularity  $\Delta X$  and valence stoichiometry  $\Delta Y$  in the samples of these ternaries. Hence, to estimate the phonon energy in an entirely ordered  $\text{CuGeSe}$  sample,  $h\nu_{p0}$ , we plot in Fig. 3 the change in  $h\nu_p$  with  $|\Delta Z|$ . Values of  $h\nu_p$  vs.  $|\Delta Z|$  for several chalcopyrite related compounds reported in the literature are also shown in this figure for comparison.

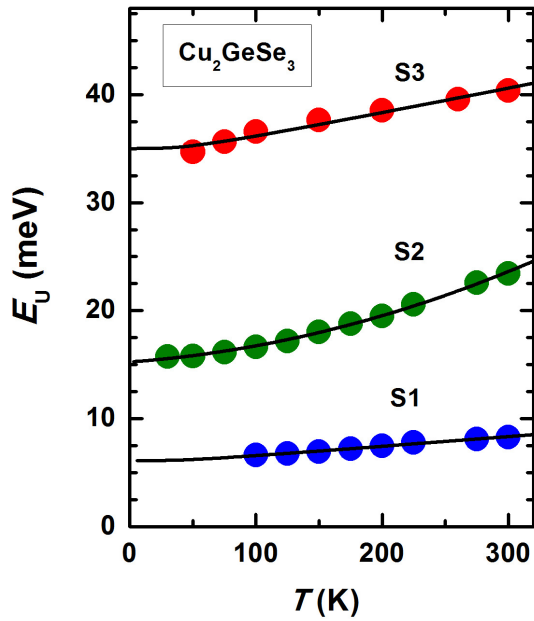


FIGURE 4. The Urbach's energy as a function of temperature for pure and Mn-doped  $\text{Cu}_2\text{GeSe}_3$  samples. The continuous curves represent a fit to the data of each sample with Eq. (4). The corresponding adjustable parameters  $P$  and  $N$  of the two different samples are given in Table II.

A linear variation between both these parameters, as expected from Eq. (3), is observed. The extrapolation of the straight line to  $|\Delta Z| = 0$ , that would correspond to a sample of ideal stoichiometry, gives  $h\nu_{p0} \approx 25$  meV ( $\bar{\nu}_{p0} \approx 201$   $\text{cm}^{-1}$ ).

From the Raman spectra of CGSe measured at 300 K reported elsewhere [26], the number of lattice vibrational modes observed is 8. The frequency of these Raman modes varies from the lowest at 135 to the highest at 385  $\text{cm}^{-1}$ . The highest intensive line, assigned as an  $A_2$ -symmetry mode, was observed at 189  $\text{cm}^{-1}$ . This is very close to  $\bar{\nu}_{p0} \approx 201$   $\text{cm}^{-1}$  estimated from Fig. 3. Also, the average frequency of the eight Raman modes observed in CGSe, weighted by the peak intensity of the lines, given in Ref. 26, is around 220  $\text{cm}^{-1}$  ( $h\nu_{p0} \approx 27$  meV) as estimated by means of the expression  $\sum_i I_i \nu_i / \sum_i I_i$ . This frequency is also in good agreement with the value calculated above.

This confirms that, apart from  $h\nu_p$  at  $\Delta Z = 0$ , additional phonon energy, proportional to  $|\Delta Z|$ , is involved in the formation of Urbach's tail in CGSe.

The variation of Urbach's energy  $E_U \equiv K_B T / s$  with temperature is shown in Fig. 4. The  $E_U$  vs  $T$  data of CGSe are fitted to Eq. (4) with  $P$  and  $N$  as adjustable parameters. A good fit, also shown in Fig. 4, is obtained with the values of  $P$  and  $N$  also given in Table II.

To calculate the Urbach's energy we have used  $\Theta \approx 200$  K. This value was obtained from a theoretical fit of the temperature dependence of the energy gap [9] by using an expression proposed by Viña *et al.* [28] based on a Bose-Einstein factor for phonons where  $\Theta$  appears as one of the

adjustable

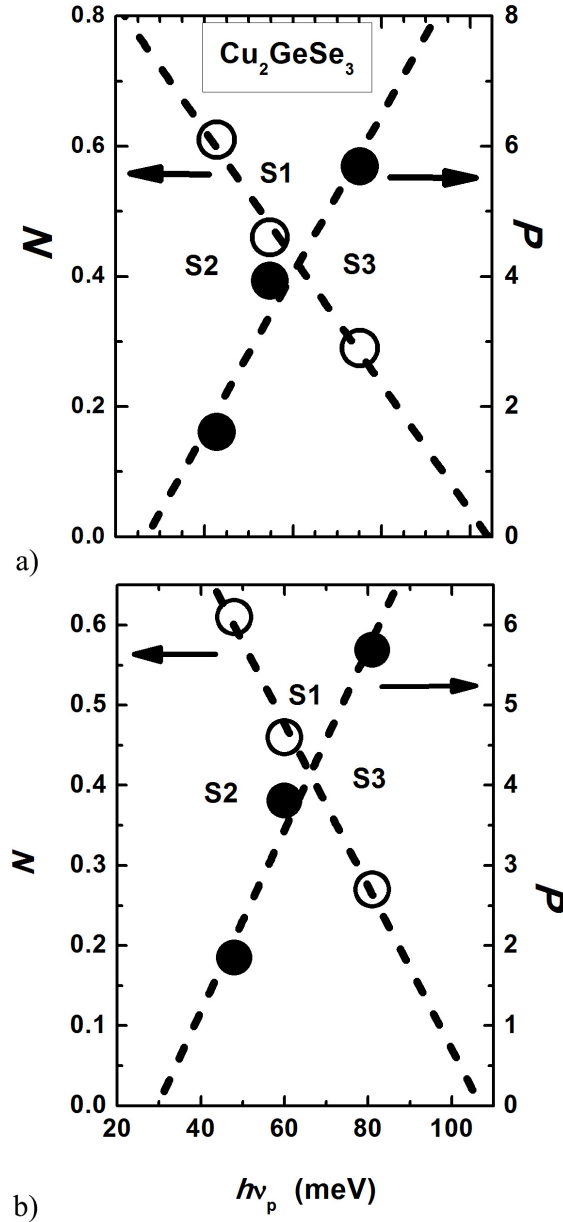


FIGURE 5. Linear variation of the parameters  $N()$  and  $P()$  on  $|\Delta Z|$  and  $h\nu_p$  for S1, S2, and S3 CGSe samples. The extrapolation of the dashed straight lines in Fig 5(b), give  $h\nu_p \approx 29$  meV at  $P = 0$  and  $h\nu_p \approx 106$  meV (1170 K) at  $N = 0$ .

parameters. It is also expected that  $P$  and  $N$  should be related to  $|\Delta Z|$  describing deviations from the ideal stoichiometry [18].

In Fig. 5(a), we plot  $P$  and  $N$  as a function of  $|\Delta Z|$ . It is observed that both  $P$  and  $N$  versus  $|\Delta Z|$  can be fitted to straight lines displaying the trend that when  $|\Delta Z|$  tends to zero, which corresponds to a defect free sample,  $P$  also approaches to zero and  $N$  to unity. The dependence of  $P$  and  $N$  on  $h\nu_p$  is also displayed in Fig. 5(b). Again, a linear dependence between both  $P$  and  $N$  vs.  $h\nu_p$  is obtained. The extrapolation of these straight lines gives  $h\nu_p \approx 29$  and

106 meV at  $P = 0$  and  $N = 0$ , respectively. The value of  $h\nu_p$  at  $P = 0$ , that would correspond to an ideal 2:1:3 CGSe sample, agrees well with both  $h\nu_p \approx 25$  meV at  $\Delta Z = 0$ , determined from the extrapolation to  $|\Delta Z| = 0$  in Fig. 3, and the average energy of all the eight optical modes, which is 27 meV. On the other hand, the value of  $h\nu_p \approx 106$  meV ( $\sim 1200$  K) at  $N = 0$ , is of the same order as the melting point of CGSe, which is about 1060 K [29,30]. This last result is consistent with the fact that CGSe undergoes an order-disorder phase transition near its melting temperature from the orthorhombic phase to a disordered face-centered cubic structure with space group  $F\bar{4}3m$  [3].

## 5. Conclusion

In the present work we report on the analysis of the Urbach's tail in  $\text{Cu}_2\text{GeSe}_3$  ternary semiconductor compound which crystallizes in an orthorhombic cell with space group  $Imm2$  ( $\frac{20}{2v}$ ). Pure and Mn-doped of  $\text{Cu}_2\text{GeSe}_3$  samples of this ma-

terial, having a small deviation from its ideal stoichiometry, were analyzed for this study. It is found that the high values of the phonon energy  $h\nu_p$  involved in the electrons and excitons-phonon interaction in the formation of this tail, which were found to be 48, 60 and 81 meV for the different  $\text{Cu}_2\text{GeSe}_3$  samples, are higher than the highest optical modes observed in this material from Raman spectra analysis, which was estimated to be about 25 meV. These high values are due to structural disorder caused by deviation from ideal stoichiometry. A relation between this energy and the parameter  $\Delta Z$ , which is the sum of the deviations from ideal molecularity and valence stoichiometry, is used in the analysis.

## Acknowledgments

This work was supported by the CDCHTA of the Universidad de los Andes (Mérida) through Project No. C-700-94-A.

- 
1. J. Y. Cho *et al.*, *J. Alloy. Compd.* **18** (2010) 506.
  2. E. J. Skoug, J. D. Cain, D. T. Morelli, *J. Alloy. Compd.* **18** (2010) 506.
  3. J. Y. Cho *et al.*, *Phys. Rev. B* **84** (2011) 085207.
  4. M. Ibáñez, *et al.*, *Chem. Mater.* **24** (2012) 4615.
  5. R. Chetty *et al.*, *Intermetallics* **54** (2014) 1.
  6. P. Qiu, X. Shi, L. Chen, *Energy Storage Materials* **3** (2016) 85.
  7. C. Coughlan *et al.*, *Chem. Rev.* **117** (2017) 5865.
  8. J. J. Lee, C. S. Yang, Y. S. Park, and K. H. Kim, *J. Appl. Phys.* **86** (1999) 2914.
  9. G. Marcano and L. Nieves, *J. Appl. Phys.* **87** (2000) 1284.
  10. G. Marcano *et al.*, *J. Appl. Phys.* **88** (2000) 822.
  11. S. G. Choi, *et al.*, *Appl. Phys. Lett.* **106** (2015) 043902.
  12. Y. Hirate *et al.*, *J. Appl. Phys.* **117** (2015) 015702.
  13. C. Rincón, G. Marcano, R. Casanova, G. E. Delgado, G. Marín, and G. Sánchez-Pérez. *Phys. Status Solidi B* **253** (2016) 697.
  14. G. Marcano, G. Sánchez-Pérez, and C. Rincón, *Physica Status Solidi B* 2017, DOI: <https://doi.org/10.1002/pssb.201700332>.
  15. F. Urbach, *Phys. Rev.* **92** (1953) 1324.
  16. M.V. Kurik, *Phys. Status Solidi A* **8** (1971) 9.
  17. G. D. Cody, T. Tiedje, B. Abeles, and Y. Goldstein, *Phys. Rev. Lett.* **47** (1981) 1480.
  18. S. M. Wasim *et al.*, *Phys. Rev. B* **64** (2001) 195101 .
  19. I. Bonalde *et al.*, *Phys. Rev. B* **69** (2004) 195201.
  20. S. M. Wasim, G. Marín, C. Rincón, G. SÁñchez-Pérez, and A. E. Mora, *J. Appl. Phys.* **83** (1998) 3318.
  21. S. H. Eom, D. J. Kim, Y.-M. Yu, Y. D. Choi, *J. Alloys Comp.* **388** (2005) 190.
  22. S. M. Wasim, G. Marín, C. Rincón, A. Rincón, L. Essaleh, *Superlattices Microstruct.*, **85** (2015) 835.
  23. S. M. Wasim, G. Marín, C. Rincón, G. SÁñchez-Pérez, *J. Appl. Phys.* **84** (1998) 5823.
  24. C. Rincón *et al.*, *J. Appl. Phys.* **90** (2001) 4423.
  25. E. Arushanov *et al.*, *Phys. Status Solidi A* **203** (2006) 2909.
  26. G. Marcano *et al.*, *Solid State Comm.* **146** (2008) 65.
  27. E. Parthé and J. Garin, *Monatsh. Chem.* **102** (1971) 1197.
  28. L. Viña, S. Logothetidis, and M. Cardona, *Phys. Rev. B* (1984) 1979.
  29. L. V. Piskach, O. V. Parasyuk, Y. E. Romanyuk, *J. Alloy Compd.* **299** (2000) 227.
  30. D. S. Prem-kumar, R. Chetty, P. Malar, and R. C. Mallik, *AIP Conference Proceedings* **1665** (2015) 120020.